

Self-Assembled Mineral Scaffolds as Model Systems for Biomineralization and Tissue Engineering

David H. Kohn^{1,2}, Kyungsup Shin², Sun-Ig Hong³, A. Champa Jayasuriya¹, Elena V. Leonova¹, Ricardo A. Rossello², Paul H. Krebsbach^{1,2}

Dept. of ¹Biologic & Materials Sciences, ²Biomedical Engineering, University of Michigan, Ann Arbor, MI,

³Dept. of Materials Science, Chungnam National University, Korea

Abstract: A system in which an organic template can self-assemble a bone-like mineral ECM analogue may regulate cell differentiation and bone formation. We functionalized 3D porous templates and exposed them to Ca and P-containing solutions to control mineral composition and morphology. Murine bone marrow stromal cells were seeded onto the scaffolds and proliferation and cytoskeletal organization were assessed. Scaffolds were implanted ectopically into nude mice and bone regeneration was assessed via histology and μ CT. Significantly more cells adhered to mineralized substrates than organic substrates. Focal adhesion contacts on non-mineralized substrates were localized at the periphery of the cell, whereas on mineralized substrates they were distributed throughout the cell surface. *In-vivo*, a significantly higher bone volume fraction was achieved in mineralized scaffolds, compared to controls. These data demonstrate the ability to controllably self-assemble 3D mineralized constructs, providing material-based control over cell function.

Keywords: Bone marrow stromal cells, biomaterial, biomineralization, regeneration, cytoskeleton

INTRODUCTION: The formation of bone from progenitor cells is variable, and controlled by factors in the local microenvironment, including the supporting biomaterial. A direct bond between a biomaterial and bone can be achieved if a bone-like mineral sheath is formed on the biomaterial surface *in-vivo* [1-3]. Therefore, a system in which an organic template can self-assemble a bone-like mineral ECM analogue *in-vitro* in a controlled manner may regulate the rate and extent of cell differentiation and bone formation, as well as provide insight into biomineralization [4]. The purpose of this study was to assess the effect of ionic strength of mineralizing solutions on mineral composition and morphology, and define the effect of self-assembled mineral on cell adhesion, cytoskeletal organization and bone formation. Specifically, *in-vivo* and *in-vitro* experiments were carried out to determine, respectively, effects of mineralization and cell seeding technique on amount and distribution of bone regenerated *in-vivo*, and the distribution of focal adhesion contacts and cell migration in tissue culture.

METHODS: Porous, 3D organic templates (85:15 poly(lactide-co-glycolide), dia = 4mm x h = 1mm, 90% porosity, pore size 250-425 μ m) were prepared by solvent casting-particulate leaching process [4]. Scaffolds were then functionalized and mineralized in simulated body fluids (SBF) [4,5] of varying ionic strength (0.75–2.0X SBF) for up to 7 days. Materials were analyzed for mineral composition and morphology via FTIR, XRD, SEM and TEM [4,5]. For cell transplantation experiments, bone marrow stromal cells (BMSC) were isolated from the femora, tibiae and humeri of 5-8 week old C57BL/6 mice. Cells (0.8×10^6 cells) were seeded into PLGA and mineralized PLGA constructs by 1 of 3 seeding techniques: 1) static seeding – cells pipetted into scaffold on 24 well-plate, 2) filtration – cells filtered into scaffold cyclically, 3) micromass seeding - cells pelleted in 5X less media than used for the other techniques and pipetted into the middle of the scaffold. Cell/scaffold constructs were implanted subcutaneously into nude mice, as previously described [6]. Constructs were harvested 6 weeks later and μ CT scanned at a threshold of 950, followed by decalcified histology. Constructs were analyzed for bone volume fraction (BVF) and bone distribution with a MatLab program. Effects of material and seeding technique on BVF were analyzed via a 2-way ANOVA.

For cell proliferation experiments, BMSCs (40,000/well) were seeded onto PLGA and mineralized PLGA substrates in 24 well plates with α -MEM + 10% FBS + 1% penicillin streptomycin. Unattached cells were washed with PBS and cells were fixed with 4% paraformaldehyde. Cell attachment was determined at 15, 30, 60 and 120 minutes by counting attached cells in 6 random low magnification fields per substrate under a light microscope. To assess cytoskeletal organization, glass cover slips were

coated with PLGA by dipping in 3.5% solution of polymer in chloroform. Half of the PLGA coated cover slips were mineralized in SBF for 5 days to deposit a layer of mineral. BMSCs were seeded on sterilized cover slips and grown for 24 hr in similar medium. Cells were fixed and focal adhesion contacts were visualized by indirect immunofluorescent localization of vinculin, using confocal microscopy. Five to ten images were randomly taken from each slide. Distances from the cell center to the focal adhesion contacts and from the cell center to the cell edge were measured for each contact. The ratio of these two measurements was used as a characteristic of the focal adhesion contact position in the cell. The average ratio for mineralized vs. non-mineralized templates was compared using a Student t-test. For the cell motility assay, mineralized and non-mineralized substrates were incubated with a suspension of colloidal gold. Unattached particles were removed, cover slips sterilized and cells seeded and grown for 24 hr. A phagokinetic index was calculated as a ratio of particle-free area to area of a cell.

RESULTS AND DISCUSSION: The composition and structure of the mineral were controllably changed with incubation time and ionic activity product. As the concentration of SBF increased, the mineral became more phosphate-rich (Fig 1); at earlier times, the mineral was carbonate-rich, and evolved into a more phosphate-rich mineral at later times. At lower ionic strengths crystals grew within the plane of the substrate, whereas at higher strengths growth was out of plane, and Ca/P ratios varied inversely with ionic strength [5]. Amorphous Ca-P was formed, with nucleation of crystalline apatite from the ACP, followed by growth of needles (100-1000 nm) along the c-axis (Fig 2).

In-vivo, a significantly higher volume fraction of regenerated bone was achieved in mineralized scaffolds compared to non-mineralized controls (Fig 3a). For a given scaffold type, filtration and micromass seeding yielded significantly greater BVF than conventional static seeding (Fig 3a). There was no significant difference in BVF between micromass seeding and filtration, but there was a significant difference in the distribution of bone between these 2 seeding methods (Fig 3b). Filtration seeding led to bone formation primarily in the periphery of the scaffold, compared to a greater amount of bone in the interior of the scaffold with micromass seeding. In culture, mineralized substrates significantly increased cell attachment (Fig. 4), caused reassembly of focal adhesion contacts (Fig. 5), and influenced cell migration as indicated by the difference in phagokinetic indices (PLGA = 3.80 ± 0.1 ; mineralized PLGA = 3.58 ± 0.08 ; $p < 0.05$). The phagokinetic index, which is modulated by cytoskeletal organization, is a negative predictor of cell attachment and spreading on a biomaterial.

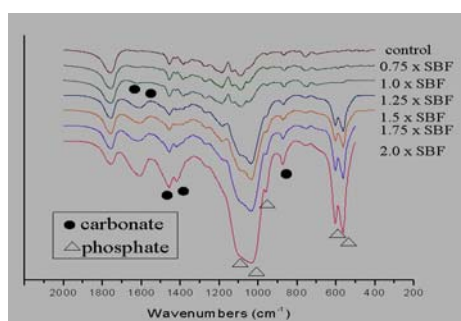


Figure 1: FTIR spectra of mineral deposited on the surface of PLGA scaffolds incubated for 16 days in solutions of varying ionic activity products

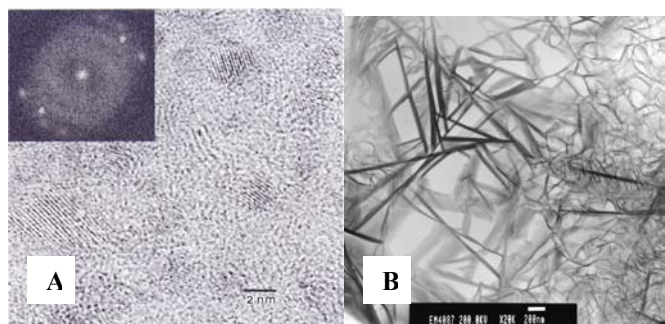


Figure 2: High resolution TEM images of A: amorphous calcium phosphate with small crystalline apatite particles; B: Needle-like ultrastructure of apatite deposits

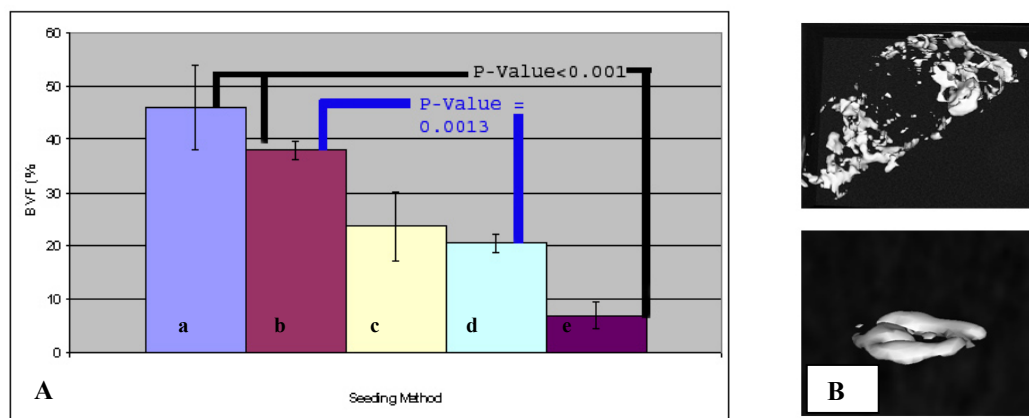


Figure 3 – A: Volume fraction of regenerated bone as a function of material and seeding technique. a: mineralized scaffold/micromass seeding; b: mineralized scaffold/filtration seeding; c: PLGA scaffold/micromass seeding; d: PLGA scaffold/filtration seeding; e: mineralized scaffold/static seeding; B: 3D micro-CT renderings of regenerated bone. top: filtration seeding, bottom: micromass seeding

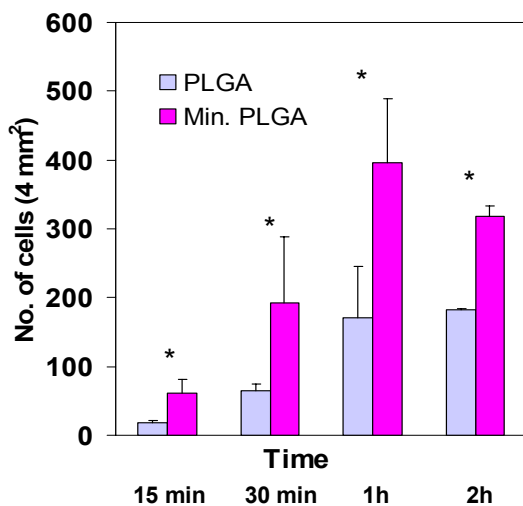


Figure 4 – BMSC attachment to mineralized vs. non-mineralized PLGA; *statistically significant at $p < 0.05$

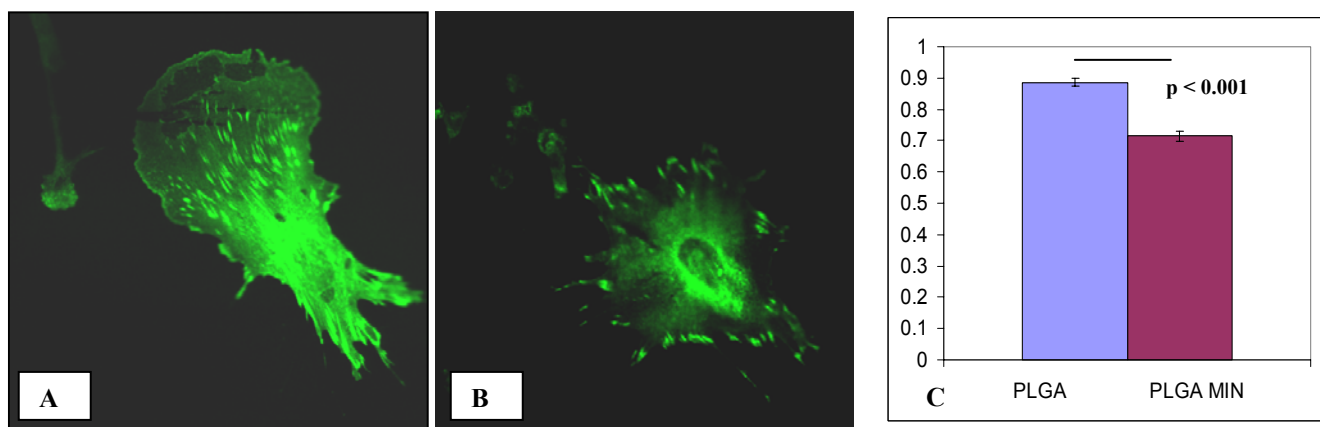


Figure 5 - Immunofluorescent localization of focal adhesion contacts using vinculin antibodies. A: mineralized PLGA distributed throughout cell surface, B: non-mineralized PLGA mostly present by cell periphery, C: ratio of distance

from cell center to focal adhesion contact vs. distance from cell center to cell edge for cells on mineralized vs. non-mineralized substrates.

A major challenge for tissue engineering is to design materials that are able to control cell function. Collectively, our data demonstrate the ability to controllably self-assemble 3D constructs consisting of an osteoconductive mineral, and provide material-based control over cell function *in-vitro* and *in-vivo*. Mineralization increased the volume fraction of regenerated bone, supporting the hypothesis that a biomimetic microenvironment will enhance cell differentiation and increase bone formation. Filtration and micromass seeding lead to a greater amount of bone regenerated, due to increased cell distribution, and cell-cell communication, respectively. Micromass seeding improved tissue regeneration in the interior of the scaffolds, a result not achieved using other more standard seeding techniques.

Understanding the mechanisms of cell-substrate interaction is critical to the design of biomaterials. Focal adhesion contacts are the specific cell-matrix adhesion sites providing the mechanical coupling of cells to the extracellular matrix. Composition of focal adhesion complexes regulates downstream signaling pathways through interaction with the cytoskeleton. These signals direct multiple cellular responses, including cell motility, proliferation and differentiation. Based on known role of focal adhesion contacts in intracellular signaling, we propose that intracellular cascades, activated in response to focal adhesion contact reassembly could trigger molecular mechanisms responsible for changes in migration and differentiation of cells on mineralized substrates.

ACKNOWLEDGEMENTS: NIH R01 DE 013380, R01 DE.015411, T32 DE 07057 and P30 AR46024, for use of the micro-CT.

REFERENCES:

- [1] Kohn, D.H. (2002). "Bioceramics." In: *Biomedical Engineers Handbook*, M. Kutz (ed.), pp. 13.1-13.24. (McGraw-Hill, New York).
- [2] Ducheyne, P. (1987). Bioceramics: material characteristics versus in vivo behavior. *J. Biomed. Mater. Res.: Appl. Biomat.* 21(A2), 219.
- [3] Nakamura, T., Yamamuro, T., Higashi, S., Kokubo, T., and Ito, S. (1985). A new glass-ceramic for bone replacement: evaluation of its bonding ability to bone tissue. *J. Biomed. Mater. Res.* 19, 685-698.
- [4] Murphy, W.L., Kohn, D.H., and Mooney, D.J. (2000). Growth of continuous bone-like mineral within porous poly(lactic-co-glycolic acid) scaffolds in-vitro. *J. Biomed. Mater. Res.* 50, 50-58.
- [5] Shin, K., Jayasuriya, A.C., and Kohn, D.H. (2003). Effect of ionic activity products on the structure and composition of mineral formed on 3-dimensional poly(lactide-co-glycolide) scaffolds. *Trans. 29th Annual Meeting Soc. for Biomat.* 29, 2003.
- [6] Kuznetsov, S.A., Krebsbach, P.H., Satomura, K., Kerr, J., Riminucci, M., Benayahu, D., and Gheron-Robey, P. (1997). Single colony derived strains of human marrow stromal fibroblasts form bone after transplantation in vivo. *J. Bone Min. Res.* 12, 1335-1347.